

Targeted Overexpression of Inducible 6-Phosphofructo-2-kinase in Adipose Tissue Increases Fat Deposition but Protects against Diet-induced Insulin Resistance and Inflammatory Responses*

Received for publication, April 9, 2012, and in revised form, May 3, 2012. Published, JBC Papers in Press, May 3, 2012, DOI 10.1074/jbc.M112.370379

Yuqing Huo^{†1,2}, Xin Guo^{§1}, Honggui Li^{§1}, Hang Xu[§], Vera Halim[§], Weiyu Zhang[¶], Huan Wang[¶], Yang-Yi Fan[§], Kuok Teong Ong^{||}, Shih-Lung Woo[§], Robert S. Chapkin[§], Douglas G. Mashek^{||}, Yanming Chen^{**}, Hui Dong^{††}, Fuer Lu^{††}, Lai Wei^{§§}, and Chaodong Wu^{§§3}

From the [†]Department of Cellular Biology and Anatomy, Georgia Health Sciences University, Augusta, Georgia 30912, the [§]Intercollegiate Faculty of Nutrition, Department of Nutrition and Food Science, Texas A&M University, College Station, Texas 77843, the [¶]Department of Medicine, University of Minnesota, Minneapolis, Minnesota, the ^{||}Department of Food Science and Nutrition, University of Minnesota, St. Paul, Minnesota, the ^{**}Department of Endocrinology, Third Affiliated Hospital of Sun Yat-sen University, Guangzhou 510630, Guangdong, China, the ^{††}Institute of Integrated Chinese and Western Medicine, Tongji Hospital, Huazhong University of Science and Technology Tongji Medical College, Wuhan 430030, HuBei, China, and the ^{§§}Institute of Hepatology, Peking University Health Science Center, Beijing 100044, China

Background: Inducible 6-phosphofructo-2-kinase links metabolic and inflammatory responses.

Results: Adipose overexpression of inducible 6-phosphofructo-2-kinase increases fat deposition, suppresses inflammatory responses, and improves insulin sensitivity in both adipose and liver tissues.

Conclusion: Inducible 6-phosphofructo-2-kinase in adipocytes uniquely dissociates diet-induced inflammatory and metabolic responses in both adipose and liver tissues.

Significance: Adipocyte-inducible 6-phosphofructo-2-kinase may underlie healthy obesity.

Increasing evidence demonstrates the dissociation of fat deposition, the inflammatory response, and insulin resistance in the development of obesity-related metabolic diseases. As a regulatory enzyme of glycolysis, inducible 6-phosphofructo-2-kinase (iPFK2, encoded by PFKFB3) protects against diet-induced adipose tissue inflammatory response and systemic insulin resistance independently of adiposity. Using aP2-PFKFB3 transgenic (Tg) mice, we explored the ability of targeted adipocyte PFKFB3/iPFK2 overexpression to modulate diet-induced inflammatory responses and insulin resistance arising from fat deposition in both adipose and liver tissues. Compared with wild-type littermates (controls) on a high fat diet (HFD), Tg mice exhibited increased adiposity, decreased adipose inflammatory response, and improved insulin sensitivity. In a parallel pattern, HFD-fed Tg mice showed increased hepatic steatosis, decreased liver inflammatory response, and improved liver insulin sensitivity compared with controls. In both adipose and liver tissues, increased fat deposition was associated with lipid profile alterations characterized by an increase in palmitoleate. Additionally, plasma lipid profiles also displayed an increase in palmitoleate in HFD-Tg mice compared with controls. In cultured 3T3-L1 adipocytes, overexpression

of PFKFB3/iPFK2 recapitulated metabolic and inflammatory changes observed in adipose tissue of Tg mice. Upon treatment with conditioned medium from iPFK2-overexpressing adipocytes, mouse primary hepatocytes displayed metabolic and inflammatory responses that were similar to those observed in livers of Tg mice. Together, these data demonstrate a unique role for PFKFB3/iPFK2 in adipocytes with regard to diet-induced inflammatory responses in both adipose and liver tissues.

Obesity is an ongoing epidemic worldwide. During obesity, fat deposition, chronic low grade inflammation, and insulin resistance are the common events that may interact with each other and bring about dysregulation of glucose and lipid metabolism in key metabolic tissues such as adipose and liver tissues (1–4). On the one hand, increased adiposity in high fat diet (HFD)⁴-fed mice is associated with adipose tissue inflammation (5, 6), which in turn contributes to the development of systemic insulin resistance. Similarly, fat deposition in hepatocytes is sufficient to trigger inflammatory responses (7, 8) and to induce liver insulin resistance by activating protein kinase C ϵ (9), whose inhibition leads to correction of liver insulin resistance

* This work was supported, in whole or in part, by National Institutes of Health Grants HL78679 and HL080569 (to Y. H.). This work was also supported by American Diabetes Association Grants 1-10-B5-76 (to Y. H.) and 1-10-JF-54 and American Heart Association Grant 12BGA9050003 (to C. W.).

[†] These authors contributed equally to this work.

² To whom correspondence may be addressed. Fax: 706-721-9799; E-mail: YHUO@georgiahealth.edu.

³ To whom correspondence may be addressed: 2253 TAMU, College Station, TX 77843. Fax: 979-862-7782; E-mail: cdwu@tamu.edu.

⁴ The abbreviations used are: HFD, high fat diet; iPFK2, inducible 6-phosphofructo-2-kinase; ACC1, acetyl-CoA carboxylase 1; FAS, fatty-acid synthase; CPT1a, carnitine palmitoyltransferase 1a; PPAR γ , peroxisome proliferator-activated receptor γ ; 6PFK1, 6-phosphofructo-1-kinase; NF- κ B, nuclear factor κ B; LFD, low fat diet; iPFK2-OX, PFKFB3/iPFK2-overexpressing; CM, conditioned medium; SCD1, stearoyl-CoA desaturase 1; SREBP1c, sterol-regulatory element-binding protein 1c; TG, triglyceride; FFA, free fatty acid; ROS, reactive oxygen species.

and improvement of insulin-stimulated adipose tissue glucose uptake (10). On the other hand, inflammation and insulin resistance are known to bring about fat deposition in hepatocytes (hepatic steatosis) (3, 11, 12), likely by increasing liver expression of genes for lipogenic enzymes such as acetyl-CoA carboxylase 1 (ACC1) and fatty-acid synthase (FAS) and decreasing liver expression of genes for fatty acid oxidation, including carnitine palmitoyltransferase 1a (CPT1a).

Recent evidence also demonstrates that fat deposition is not necessarily associated with increased insulin resistance and inflammatory responses. In female mice, elevating endogenous circulating levels of adiponectin brings about an increase in body fat and improves glucose tolerance (13). As additional evidence, treatment of HFD-fed wild-type mice with rosiglitazone, a peroxisome proliferator-activated receptor γ (PPAR γ) agonist, increases adiposity but decreases adipose tissue proinflammatory response (14), supporting the dissociation of adiposity and adipose tissue inflammatory response. Similarly, the dissociation of hepatic steatosis and liver inflammatory response and insulin sensitivity is observed in genetically modified mice. Upon targeted overexpressing human acyl-CoA:diacylglycerol acyltransferase in the liver, the transgenic mice exhibit an increase in hepatic steatosis, yet display normal glucose tolerance and systemic insulin sensitivity and normal liver inflammatory response (15). When malonyl-CoA-insensitive CPT1a (mCPT1a) is overexpressed in the liver in both diet-induced and genetically obese mice, the liver inflammatory response decreases independently of hepatic steatosis (16). Precisely how fat deposition alters inflammatory responses and insulin signaling in both adipose and liver tissues in opposite ways is not fully understood, but it may be attributable to the composition of fat deposited rather than the amount of fat deposition (16).

PFKFB3 encodes for inducible 6-phosphofructo-2-kinase (iPKF2), whose product fructose 2,6-bisphosphate is the most powerful activator of glycolytic enzyme 6-phosphofructo-1-kinase (17–19). Recent evidence demonstrates that global disruption of PFKFB3/iPKF2 blunts diet-induced adiposity but exacerbates adipose tissue inflammatory response and systemic insulin resistance (20). Additionally, PFKFB3/iPKF2 is involved in the anti-inflammatory and anti-diabetic effects of PPAR γ activation likely by promoting fat synthesis in adipose tissue (21). At the cellular level, PFKFB3/iPKF2 increases adipocyte glycolysis and glycolysis-driven lipogenesis. This in turn suppresses oxidative stress by channeling fatty acids from excessive oxidation to fat synthesis, thereby inhibiting inflammatory signaling from the nuclear factor- κ B (NF- κ B) and c-Jun N-terminal kinase 1 (JNK1) pathways. However, the role of PFKFB3/iPKF2 in adipocytes in dissociating fat deposition, inflammation, and insulin resistance at the systemic level in mice is not known. It is also not clear if adipocyte PFKFB3/iPKF2 influences adipose tissue to alter liver metabolic and inflammatory responses. This study provides evidence supporting a unique role for PFKFB3/iPKF2 in adipocytes in the dissociation of diet-induced inflammatory responses and fat deposition in both adipose and liver tissues.

EXPERIMENTAL PROCEDURES

Animal Experiments—Mice (C57BL/6J background) that selectively overexpressed PFKFB3/iPKF2 in adipose tissue (Adi-PFKFB3TG, Tg) were generated using aP2-PFKFB3 cDNA transgene based on published literature (22, 23). Wild-type (WT) littermates were used as controls. All mice were maintained on a 12:12-h light/dark cycle (lights on at 06:00). At 5–6 weeks of age, male mice were fed an HFD (60% fat calories, 20% protein calories, and 20 carbohydrate calories) or a low fat diet (LFD) (10% fat calories, 20% protein calories, and 70 carbohydrate calories) for 12 weeks as described previously (20, 21). After the feeding regimen, mice were fasted for 4 h before sacrifice for collection of blood and tissue samples (24–26). Epididymal, mesenteric, and perinephric fat depots were dissected and weighed as visceral fat content (25). After weighing, adipose tissue and liver samples were either fixed and embedded for histological and immunohistochemical analyses or frozen in liquid nitrogen and stored at -80°C for further analyses. Some mice were fasted similarly and used for insulin and glucose tolerance tests, very low density lipoprotein (VLDL)-triglyceride secretion assay, and insulin signaling analyses. All study protocols were reviewed and approved by the Institutional Animal Care and Use Committee of Texas A&M University.

Confirmation of PFKFB3/iPKF2 Overexpression—Genomic DNA was prepared from mouse tail samples and subjected to PCR analyses using primers located within the aP2 promoter and PFKFB3 exon 2 (aP2-PFKFB3) or primers for casein. The amount of iPKF2 in white adipose tissue, liver, muscle, and bone marrow samples was determined using Western blot analyses (20, 21).

Insulin and Glucose Tolerance Tests—Mice were fasted for 4 h and intraperitoneally injected with insulin (0.5 units/kg for LFD-fed mice and 1 unit/kg for HFD-fed mice) or D-glucose (2 g/kg). For insulin tolerance tests, blood samples (5 μl) were collected from the tail vein before and at 15, 30, 45, and 60 min after the bolus insulin injection. Similarly, for glucose tolerance tests, blood samples were collected from the tail vein before and at 30, 60, 90, and 120 min after the glucose bolus injection (20, 21).

Very Low Density Lipoprotein (VLDL)-Triglyceride Release—After the feeding regimen, HFD-fed mice were fasted for 5 h and injected with tyloxapol (500 mg/kg, i.v.). Plasma levels of triglycerides were measured in blood samples taken at 20, 40, 60, and 80 min after the injection (27).

Measurement of Metabolic Parameters—The levels of plasma glucose, triglycerides, and free fatty acids, as well as hepatic triglycerides, were measured using metabolic assay kits (Sigma and BioVision, Mountain View, CA). The levels of plasma insulin and leptin were measured using ELISA kits (Crystal Chem Inc., Downers Grove, IL).

Histological and Immunohistochemical Analyses—The paraffin-embedded adipose tissue and liver blocks were cut into sections of 5 μm thickness and stained with H&E. In addition, sections were stained for the expression of cell (macrophage) surface marker (F4/80) with rabbit anti-F4/80 (1:100) (AbD Serotec, Raleigh, NC) as described previously (20, 21). The frac-

Adipocyte iPFK2 Dissociates Inflammation from Fat Deposition

tion of F4/80-expressing cells for each sample was calculated as the sum of the number of nuclei of F4/80-expressing cells divided by the total number of nuclei in sections of each sample. Six fields per slide were included, and a total of 4–6 mice per group were examined.

Cell Culture and Treatment—Stable PFKFB3/iPFK2-overexpressing (iPFK2-OX) adipocytes and green fluorescent protein (GFP)-expressing adipocytes (control) were established and maintained as described previously (21). Adipocyte-conditioned medium was collected at 8–10 days post-differentiation and used to treat mouse primary hepatocytes as described below. To determine rates of [14 C]glucose incorporation into lipid, each well (6-well plate) of differentiated adipocytes was incubated with DMEM supplemented with 1 μ Ci of [U- 14 C]-glucose for 24 h (20). To examine the status of adipocyte oxidative stress, cells were treated with palmitate (250 μ M) or bovine serum albumin (BSA) for 24 h and used to measure the production of reactive oxygen species (ROS) using the nitro blue tetrazolium assay as described previously (20, 21). To quantify adipocyte gene expression, total RNA of the cells was prepared and used for real time RT-PCR. To determine changes in inflammatory signaling, cells were treated with or without palmitate (250 μ M) for 24 h prior to harvest. Cell lysates were prepared and used to measure the levels of NF- κ B p65 and phospho-p65 (Ser-468) using Western blots. To determine changes in insulin signaling, cells were treated with or without insulin (100 nM) for 30 min prior to harvest. Cell lysates were prepared and used to measure the levels of Akt1/2 and phospho-Akt (Ser-473) using Western blots.

Mouse primary hepatocytes were isolated as described previously (25, 28). To address direct effects of adipocyte factors generated in response to PFKFB3/iPFK2 action, isolated WT hepatocytes were treated with iPFK2-OX-adipocyte-conditioned medium (iPFK2-OX-CM) or GFP-expressing adipocyte-conditioned medium (GFP-CM, control) in M199 medium at a 1:1 ratio for 48 h in the presence or absence of palmitate (250 μ M) for the last 24 h. Hepatocyte lipid accumulation was analyzed using Oil Red O staining and the colorimetric assay to quantify triglyceride content. Hepatocyte ROS production, gene expression, inflammatory, and insulin signaling were analyzed as described above.

Lipid Profiling—Total lipids from adipose and liver tissue, as well as plasma and adipocyte-conditioned medium were extracted using chloroform/methanol (2:1, v/v) and separated by thin layer chromatography. Lipid fractions were analyzed by capillary gas chromatography (28, 29).

RNA Isolation, Reverse Transcription, Real Time PCR, and Microarray—Total RNA was isolated from frozen tissue samples and cultured/isolated cells. RNA isolation and real time RT-PCR were conducted as described previously (20, 21). The mRNA levels were analyzed for ACC1, FAS, stearoyl-CoA desaturase 1 (SCD1), sterol-regulatory element-binding protein 1c (SREBP1c), PPAR γ , hormone-sensitive lipase, IL-6, TNF α , carbohydrate-responsive element-binding protein, CPT1a, liver fatty acid-binding protein, VLDL receptor, and/or apoB.

Western Blots—Lysates were prepared from frozen tissue samples and cultured cells. Western blots were conducted as described previously (25, 26). The levels of iPFK2, Akt1/2,

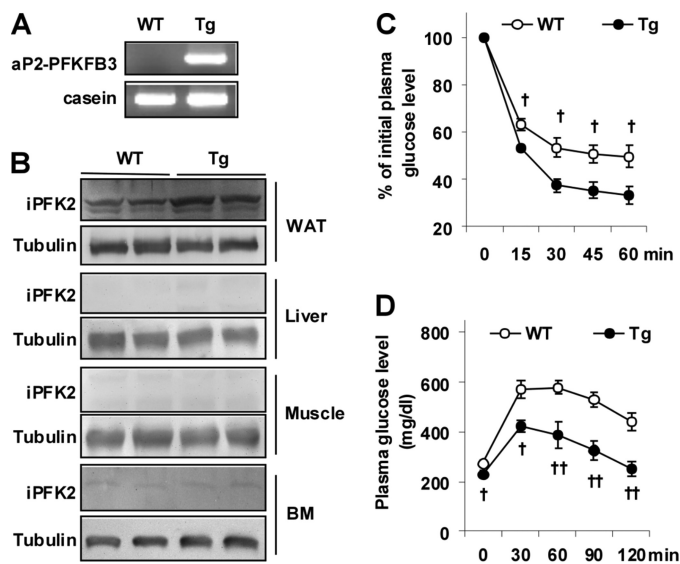


FIGURE 1. Selective overexpression of PFKFB3/iPFK2 in adipose tissue protects mice from diet-induced insulin resistance. *A*, genomic DNA was prepared from Adi-PFKFB3TG (Tg) mice and wild-type littermates and used for PCR analyses of aP2-PFKFB3 transgene. *B*, iPFK2 (encoded by PFKFB3) abundance in white adipose tissue (WAT), liver, skeletal muscle, and bone marrow (BM) was measured using Western blots. *C*, insulin tolerance tests. *D*, glucose tolerance tests. *C* and *D*, male Tg mice and WT mice, at 5–6 weeks of age, were fed an HFD for 12 weeks. After the feeding regimen, HFD-fed mice were fasted for 4 h and received an intraperitoneal injection of insulin (1 unit/kg) (*C*) or glucose (2 g/kg) (*D*). Data are means \pm S.E., $n = 6–10$. \dagger , $p < 0.05$; $\dagger\dagger$, $p < 0.01$ Tg versus WT at the same time point.

phospho-Akt (Ser-473), NF- κ B p65, and phospho-p65 (Ser-468) were quantified.

Statistical Methods—Data are presented as means \pm S.E. Statistical significance was assessed by unpaired two-tailed analysis of variance or Student's *t* test. Differences were considered significant at the two-tailed $p < 0.05$.

RESULTS

Overexpression of PFKFB3/iPFK2 in Adipose Tissue Protects against HFD-induced Insulin Resistance—PFKFB3/iPFK2 dissociates insulin resistance from diet-induced adiposity and is involved in the anti-diabetic effect of PPAR γ activation (20, 21). To address a direct role for the PFKFB3/iPFK2 in adipocytes, we analyzed aspects of diet-induced inflammatory and metabolic responses in Tg mice (Fig. 1*A*). In confirmatory experiments, PFKFB3/iPFK2 overexpression was targeted to adipose tissue, but not in liver, muscle, or bone marrow (Fig. 1*B*). Thus, Tg mice used herein overexpressed PFKFB3 selectively in adipose tissue. On an LFD, Tg mice did not differ significantly from WT mice in major metabolic parameters (Table 1), although a slight increase in body weight was observed (data not shown). In contrast, on an HFD, Tg mice displayed a much smaller increase in the severity of HFD-induced systemic insulin resistance and glucose intolerance (Fig. 1, *C* and *D*), as well as hyperglycemia and hyperinsulinemia (Table 1). Therefore, selective overexpression of PFKFB3/iPFK2 in adipose tissue protects mice from diet-induced systemic insulin resistance and metabolic dysregulation.

Overexpression of PFKFB3/iPFK2 in Adipose Tissue Dissociates Adipose Tissue Inflammatory Response and Insulin Resistance from Diet-induced Adiposity—Feeding an HFD to mice induces adiposity and adipose tissue inflammation (3, 30),

TABLE 1

Plasma parameters in Tg and WT mice

Male Adi-PFKFB3TG (Tg) mice and wild-type (WT) littermates, at 5–6 weeks of age, were fed an HFD or LFD for 12 weeks. After the feeding regimen, mice were fasted for 4 h before collection of blood samples. Data are means \pm S.E., $n = 6$ –10.

	WT	Tg
Glucose (mg/dl)		
LFD	177 \pm 5	153 \pm 10
HFD	264 \pm 9 ^a	208 \pm 15 ^{b,c}
Insulin (ng/ml)		
LFD	2.6 \pm 0.4	2.2 \pm 0.2
HFD	4.7 \pm 0.6 ^b	2.7 \pm 0.4 ^c
Leptin (ng/ml)		
LFD	5.3 \pm 0.9	26.7 \pm 1.2 ^d
HFD	58.6 \pm 10.1 ^a	91.6 \pm 8.5 ^{a,c}
Free fatty acids (mM)		
LFD	0.4 \pm 0	0.5 \pm 0.1
HFD	0.6 \pm 0.1 ^b	0.5 \pm 0.1
Triglycerides (mg/dl)		
LFD	39 \pm 0	38 \pm 1
HFD	42 \pm 1 ^b	41 \pm 1

^a $p < 0.01$ HFD versus LFD for the same genotype.

^b $p < 0.05$ HFD versus LFD for the same genotype.

^c $p < 0.05$ Tg versus WT for the same diet.

^d $p < 0.01$ Tg versus WT for the same diet.

which are considered to be critical factors contributing to systemic insulin resistance. On an HFD, Tg mice exhibited a significant increase in body weight but showed no difference in food intake compared with WT littermates (data not shown). In addition, Tg mice exhibited a greater increase in fat mass and adiposity (Fig. 2, A and B). Consistently, adipocytes in Tg mice were much enlarged compared with WT mice (Fig. 2C). Compared with controls, adipose tissue of HFD-fed Tg mice accumulated more macrophages (Fig. 2, D and E) but showed a significant decrease in NF- κ B p65 (Ser-468) phosphorylation (Fig. 2F), indicating a decrease in adipose tissue inflammatory response. In parallel, adipose tissue expression of genes for lipid accumulation was increased, whereas adipose tissue expression of proinflammatory cytokines was decreased (Fig. 2G). When insulin signaling was analyzed, insulin-stimulated Akt (Ser-473) phosphorylation was increased in adipose tissue of Tg mice compared with WT mice (Fig. 2H). Together, these results suggest that overexpression of PFKFB3/iPFK2 in adipose tissue suppresses diet-induced adipose tissue inflammatory response and insulin resistance while promoting fat deposition in adipose tissue.

Overexpression of PFKFB3/iPFK2 in Adipose Tissue Dissociates Liver Inflammatory Response and Insulin Resistance from Diet-induced Hepatic Steatosis—Feeding an HFD to mice also induces hepatic steatosis, as well as liver inflammatory response and insulin resistance (3, 30, 31). To determine the role of PFKFB3/iPFK2 in adipocytes with respect to the regulation of diet-induced liver metabolic and inflammatory response, aspects of liver responses were analyzed. Consistent with increased adiposity (Fig. 2), Tg mice exhibited a greater increase in liver weight and in the severity of diet-induced hepatic steatosis than controls (Fig. 3, A–C). Additionally, the expression of liver genes for lipogenesis, including ACC1, FAS, SREBP1c, and carbohydrate-responsive element-binding protein in HFD-fed Tg mice, was increased compared with controls (Fig. 3D). In contrast, hepatic expression of key genes involved in fatty acid oxidation, fatty acid uptake, and VLDL-

triglyceride secretion in HFD-fed Tg mice did not differ from that in WT mice. Additionally, rates of VLDL-triglyceride release in HFD-fed Tg were comparable with those in WT mice (Fig. 3E). Thus, selective overexpression of PFKFB3/iPFK2 in adipose tissue promotes fat deposition in the liver, due largely to an increase in hepatic lipogenesis. When liver inflammatory response was assessed, livers in HFD-fed Tg mice accumulated fewer macrophages/Kupffer cells than controls (Fig. 3, F and G). Additionally, HFD-fed Tg mice exhibited a slight but significant decrease in liver NF- κ B p65 (Ser-468) phosphorylation (Fig. 3H), which was accompanied by a greater decrease in liver proinflammatory cytokine expression (Fig. 3I). In contrast, HFD-fed Tg mice showed a marked increase in liver Akt (Ser-473) phosphorylation at both basal and insulin-stimulated conditions compared with WT mice (Fig. 2J). Together, these results indicate that selective overexpression of PFKFB3/iPFK2 in adipose tissue protects mice from diet-induced liver inflammatory response and insulin resistance while promoting hepatic steatosis.

Overexpression of PFKFB3/iPFK2 in Adipose Tissue Alters Tissue and Plasma Lipid Profiles—Given that PFKFB3/iPFK2 overexpression in adipose tissue promotes fat deposition and that fat composition but not fat content determines tissue proinflammatory status and insulin sensitivity (16, 32), the lipid profiles in both adipose and liver tissues were analyzed. Compared with controls, the levels of palmitoleate, a putative anti-inflammatory unsaturated fatty acid (32), were increased in both TG and FFA isolated from HFD-fed Tg mouse adipose tissue (Fig. 4, A and B). Interestingly, the levels of palmitate were increased in adipose tissue TGs (Fig. 4A). Similarly, the levels of palmitoleate were increased in both TG and FFA isolated from livers of HFD-fed Tg mice compared with HFD-fed WT mice (Fig. 4, C and D). Compared with controls, the levels of oleate, another monounsaturated fatty acid, were also increased in both liver TG and FFA fractions in HFD-fed Tg mice (Fig. 4, C and D). Consistent with an increase in the levels of palmitoleate, the expression of SCD1 along with the expression of other key lipogenic genes, including FAS and SREBP1c, were increased in both adipose and liver tissues (Fig. 2G and Fig. 3D). Because PFKFB3/iPFK2 overexpression did not occur in livers, plasma lipid profile was also analyzed to address a potential link between adipose and liver tissues. Compared with controls, only the levels of palmitoleate in HFD-fed Tg mice were increased (Fig. 4E). In combination, these results suggest that selective overexpression of PFKFB3/iPFK2 in adipose tissue promotes deposition of unsaturated fatty acids.

PFKFB3/iPFK2 Overexpression Dissociates Adipocyte Inflammatory Response and Insulin Resistance from Fat Deposition—To verify a direct role for PFKFB3/iPFK2 in dissociating the inflammatory response and insulin resistance linked to fat deposition, stable adipocytes overexpressing PFKFB3/iPFK2 (iPFK2-OX) were established (Fig. 5A). Compared with GFP-expressing adipocytes (control), iPFK2-OX adipocytes exhibited an increase in rates of glucose incorporation into lipid (Fig. 5B). Consistently, the expression of key lipogenic genes, including FAS, SCD1, and SREBP1c, was increased in iPFK2-OX adipocytes compared with controls (Fig. 5C). While accumulating more lipids (data not shown), iPFK2-OX showed a decrease in

Adipocyte iPFK2 Dissociates Inflammation from Fat Deposition

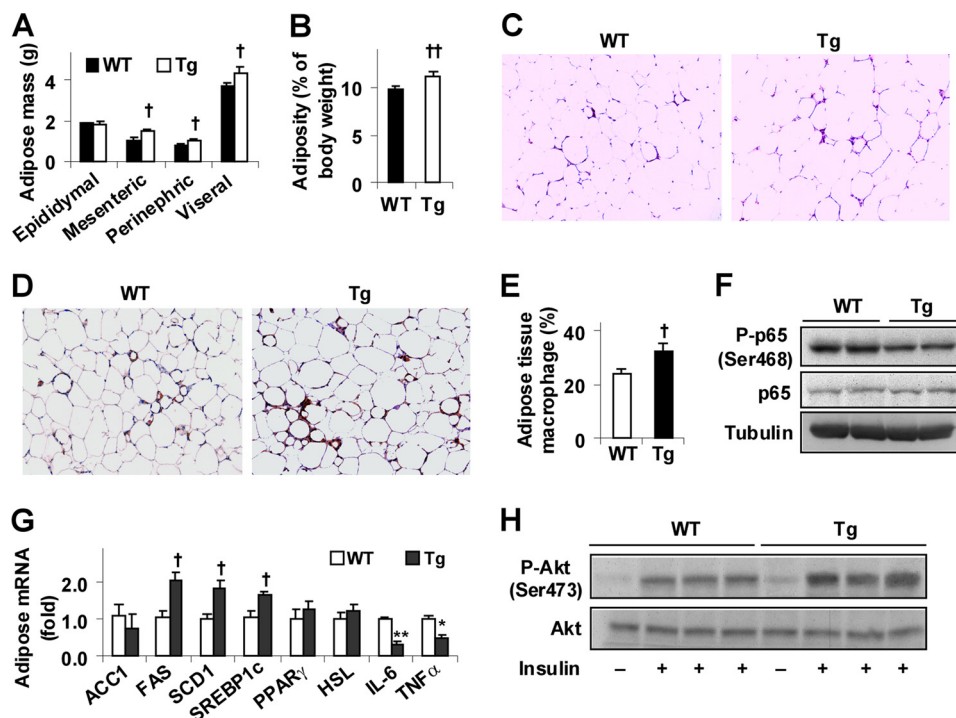


FIGURE 2. Overexpression of PFKFB3/iPFK2 in adipose tissue decreases diet-induced adipose tissue inflammatory response and improves insulin signaling while increasing adiposity. At 5–6 weeks of age, male Tg and WT mice were fed an HFD for 12 weeks. *A*, changes in fat mass. Visceral fat content was estimated from the sum of epididymal, perinephric, and mesenteric fat mass. *B*, changes in adiposity. *C*, adipose tissue histology. The sections of epididymal fat pad were stained with hematoxylin and eosin (10 \times). *D*, macrophage infiltration in adipose tissue. The sections of epididymal fat pad were immunostained for F4/80. *E*, fraction of adipose tissue macrophages. *F*, adipose tissue inflammatory signaling. The levels of NF- κ B p65 and phospho-p65 (Ser-468) were examined using Western blot analyses. *G*, adipose tissue gene expression was quantified using real time RT-PCR. *H*, adipose tissue insulin signaling. Tissue samples of HFD-fed mice were collected at 5 min after a bolus injection of insulin (1 unit/kg) or PBS into the portal vein. The levels of Akt1/2 and phospho-Akt (Ser-473) were examined using Western blot analyses. *A*, *B*, *E*, and *G*, data are means \pm S.E., $n = 6$ –10. \dagger , $p < 0.05$; \ddagger , $p < 0.01$ Tg versus WT (*B* and *E*) for the same fat pad (*A*) and for the same gene (*G* for an increase); *, $p < 0.05$; **, $p < 0.01$ Tg versus WT for the same gene (*G* for a decrease).

the generation of reactive oxygen species (ROS) under both basal (BSA) and palmitoleate-stimulated conditions (Fig. 5*D*), indicating decreased the status of oxidative stress. Additionally, iPFK2-OX adipocytes showed a decrease in NF- κ B p65 (Ser-468) phosphorylation (Fig. 5*E*), as well as IL-6 expression in both basal (PBS) and TNF α -stimulated conditions compared with controls (Fig. 5*F*). When insulin signaling was analyzed, iPFK2-OX adipocytes showed an increase in Akt (Ser-473) phosphorylation at both basal and insulin-stimulated conditions compared with control adipocytes (Fig. 5*G*). Thus, PFKFB3/iPFK2 has direct effects on decreasing adipocyte inflammatory response and on improving insulin signaling while increasing fat deposition.

To verify if PFKFB3/iPFK2 overexpression directly stimulates adipocyte production of palmitoleate, the lipid profile of adipocyte-CM was analyzed. Compared with controls, the levels of palmitoleate in iPFK2-OX-CM were significantly increased (Fig. 5*H*). This increase was associated with the increased adipocyte expression of SCD1 in iPFK2-OX adipocytes (Fig. 5*C*) and is consistent with increased levels of palmitoleate in plasma isolated from HFD-fed Tg mice (Fig. 4*E*). Together, these data provide the first evidence in support of a role for PFKFB3/iPFK2, a regulator of adipocyte glycolysis, in stimulating adipocyte production of palmitoleate.

Adipocyte-derived Factors Dissociate Hepatocyte Inflammatory Response and Insulin Resistance from Fat Deposition—To

address the direct effects of adipocyte factors generated in response to PFKFB3/iPFK2 overexpression on hepatocyte metabolic and inflammatory responses, adipocyte-conditioned medium was used to treat WT mouse primary hepatocytes as described previously (11, 33, 34). Palmitate was supplemented into hepatocyte medium to induce fat deposition and inflammatory responses. Compared with controls, treatment with iPFK2-OX-CM markedly increased hepatocyte fat deposition (Fig. 6*A*) but decreased hepatocyte production of ROS at both basal and palmitate-stimulated conditions (Fig. 6*B*). Additionally, NF- κ B p65 (Ser-468) phosphorylation in hepatocytes treated with iPFK2-OX-CM was much lower than in hepatocytes treated with control medium (Fig. 6*C*). Consistent with changes in hepatocyte fat deposition and inflammatory responses, the expression of FAS and SREBP1c was increased, whereas the expression of IL-6 and TNF α was decreased in hepatocytes treated with iPFK2-OX-CM compared with hepatocytes treated with control medium (Fig. 6*D*). When insulin signaling was analyzed, hepatocytes treated with iPFK2-OX-CM showed a significant increase in Akt (Ser-473) phosphorylation at both basal and insulin-stimulated conditions compared with control hepatocytes (Fig. 6*E*). In combination, these results suggest that adipocyte-derived factors generated in response to PFKFB3/iPFK2 overexpression directly dissociate hepatocyte inflammatory response and insulin resistance from fat deposition.

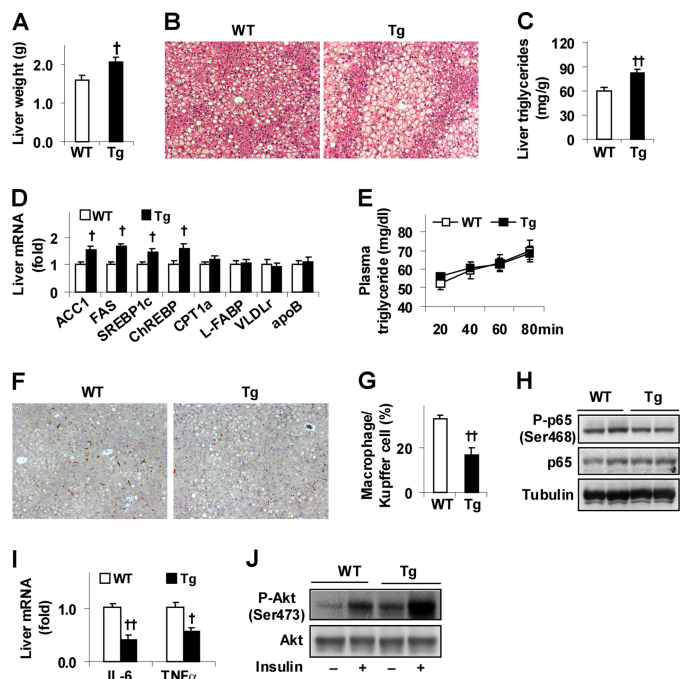


FIGURE 3. Overexpression of PFKFB3/iPFK2 in adipose tissue decreases diet-induced liver inflammatory response and improves insulin signaling while increasing hepatic steatosis. At 5–6 weeks of age, male Tg and WT mice were fed an HFD for 12 weeks. *A*, changes in liver weight. *B*, liver histology. Liver sections were stained with hematoxylin and eosin (10 \times). *C*, levels of hepatic triglycerides were quantified using the biochemical assay. *D*, liver gene expression was quantified using real time RT-PCR. *E*, VLDL-triglyceride secretion. HFD-fed mice were fasted for 5 h and injected with tyloxapol (500 mg/kg, i.v.). Plasma levels of triglycerides were measured in blood samples taken at the indicated time points after the injection. *F*, liver macrophages/Kupffer cells. Liver sections were immunostained for F4/80. *G*, fraction of liver macrophages/Kupffer cells. *H*, liver inflammatory signaling. The levels of NF- κ B p65 and phospho-p65 (Ser-468) were examined using Western blot analyses. *I*, liver expression of proinflammatory cytokines was quantified using real time RT-PCR. *J*, liver insulin signaling. Tissue samples of HFD-fed mice were collected at 5 min after a bolus injection of insulin (1 unit/kg) or PBS into the portal vein. The levels of Akt1/2 and phospho-Akt (Ser-473) were examined using Western blot analyses. *A*, *C*–*E*, *G*, and *I*, data are means \pm S.E., $n = 6$ – 10 . \dagger , $p < 0.05$; $\dagger\dagger$, $p < 0.01$ Tg versus WT (*A*, *C*, and *G*) for the same gene (*D* and *I*).

DISCUSSION

Although it is commonly accepted that a vicious cycle exists within fat deposition, the inflammatory response, and insulin resistance, increasing evidence also indicates that these metabolic and inflammatory events can be dissociated (13–16, 35). As additional evidence, global disruption of PFKFB3/iPFK2 blunts diet-induced adiposity but exacerbates adipose tissue inflammatory response and systemic insulin resistance (20). Given the important role for adipose tissue in regulating systemic metabolic and inflammatory responses (23, 36), we hypothesized that adipocyte PFKFB3/iPFK2 directs the dissociation of the inflammatory response and insulin resistance associated with fat deposition locally in adipose tissue and distally in the liver. To test this hypothesis, this study examined HFD-induced metabolic and inflammatory events in Tg mice and wild-type littermates. Upon treating mouse primary hepatocytes with adipocyte-conditioned medium, the effects of adipocyte factors generated in response to PFKFB3/iPFK2 overexpression on hepatocyte metabolic and inflammatory responses were also determined.

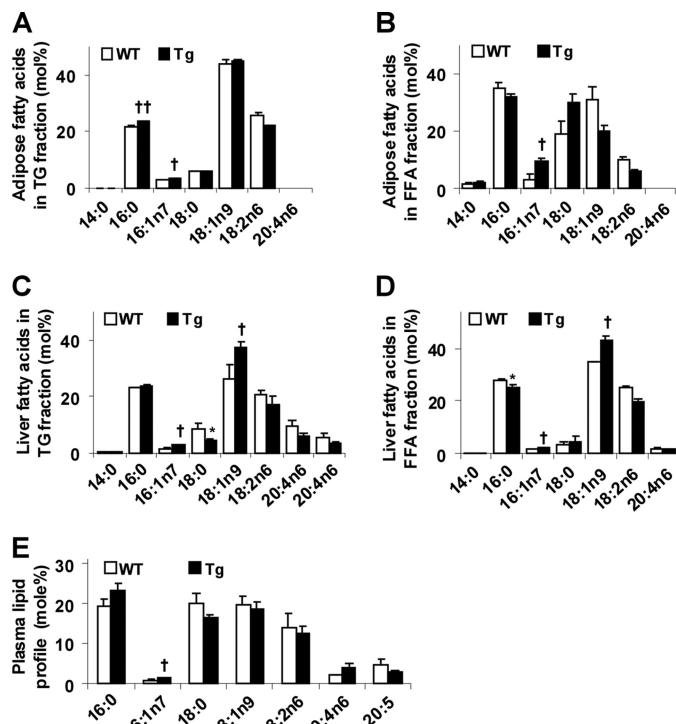


FIGURE 4. Overexpression of PFKFB3/iPFK2 in adipose tissue alters lipid profiles in adipose, liver, and plasma. At 5–6 weeks of age, male Tg and WT mice were fed an HFD for 12 weeks. *A*, lipid profile in triglycerides fractionated from adipose tissue samples. *B*, lipid profile in fatty acids fractionated from adipose tissue samples. *C*, lipid profile in triglycerides fractionated from liver samples. *D*, lipid profile in fatty acids fractionated from liver samples. *E*, plasma lipid profile. *A*–*E*, data are means \pm S.E., $n = 4$ – 6 . \dagger , $p < 0.05$; $\dagger\dagger$, $p < 0.01$ Tg versus WT for the same fatty acid (*A*–*E* for an increase); $*$, $p < 0.05$ Tg versus WT (*C* and *D* for a decrease).

As a result of selective PFKFB3/iPFK2 overexpression in adipose tissue, Tg mice exhibited a dissociation of fat deposition, the inflammatory response, and insulin resistance. Locally, adiposity in HFD-fed Tg mice was greater than in wild-type littermates, which is consistent with the role of PFKFB3/iPFK2 in promoting glycolysis and glycolysis-derived lipogenesis as indicated by the results from PFKFB3/iPFK2-overexpressing adipocytes. However, while showing increased adiposity, HFD-fed Tg mice exhibited a decrease in adipose tissue NF- κ B p65 (Ser-468) phosphorylation and proinflammatory cytokine expression while accumulating more macrophages. This phenotype was nearly identical to that observed in adipose tissue of wild-type mice upon treatment with rosiglitazone (14, 21). Because *aP2*-PFKFB3 primarily elevated PFKFB3/iPFK2, it is postulated that PFKFB3/iPFK2 is capable of mediating a dissociation of fat deposition and the inflammatory response. In support of this finding, PFKFB3/iPFK2 overexpression in adipocytes increased fat accumulation but decreased adipocyte inflammatory response. Previous evidence from rosiglitazone-treated adipocytes suggests that PFKFB3/iPFK2 channels fatty acids from excessive oxidation to synthesis, thereby reducing adipocyte ROS production and the inflammatory response while increasing fat accumulation. This is also the case in PFKFB3/iPFK2-overexpressing adipocytes. Additionally, PFKFB3/iPFK2 overexpression increased SCD1 expression in both adipose tissue and adipocytes, which appeared to alter the lipid profile in adipose tissue of Tg mice and in conditioned medium of PFKFB3/

Adipocyte iPFK2 Dissociates Inflammation from Fat Deposition

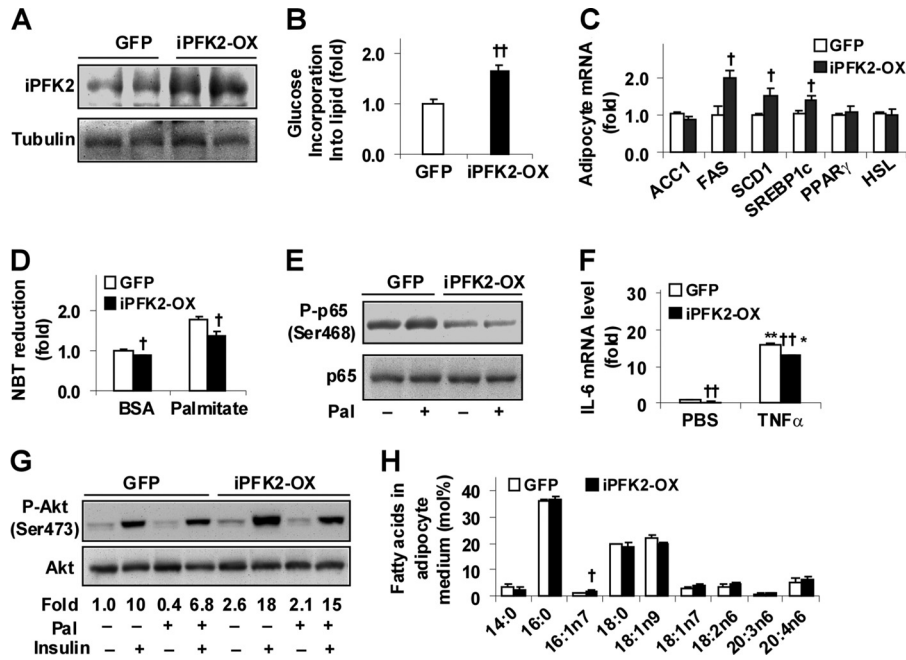


FIGURE 5. PFKFB3/iPFK2 overexpression decreases adipocyte inflammatory response and improves insulin signaling while increasing fat deposition. Stable iPFK2-OX adipocytes and GFP-expressing adipocytes were established and subjected to metabolic and inflammatory assays. Each of the assays was performed at least in quadruplicate. *A*, amounts of iPFK2 in cells lysates were examined using Western blot analyses. *B*, changes in the rates of glucose incorporation into lipid. *C*, adipocyte gene expression was quantified using real time RT-PCR. *D*, production of ROS was measured using the nitro blue tetrazolium (*NBT*) assay. *E*, adipocyte inflammatory signaling. The levels of NF- κ B p65 and phospho-p65 (Ser-468) were examined using Western blot analyses. *F*, adipocyte expression of IL-6. *G*, adipocyte insulin signaling. Prior to harvest, adipocytes were incubated with or without insulin (100 nM) for 30 min. Phospho-Akt (Ser-473) to Akt1/2 ratios were calculated using densitometry and expressed as fold changes. *D–G*, adipocytes were incubated with or without palmitate (250 μ M) for 24 h (*D*, *E*, and *G*) or TNF α (10 ng/ml) for 6 h (*F*). *H*, lipid profile of adipocyte-conditioned medium. iPFK2-OX adipocytes and GFP-expressing 3T3-L1 were differentiated for 10 days before collection of conditioned medium. *B–D*, *F*, and *H*, †, $p < 0.05$; ††, $p < 0.01$ iPFK2-OX versus GFP (*B*) for the same gene (*C*) under the same condition (*D* and *F*) and for the same fatty acid (*H*). *, $p < 0.05$; **, $p < 0.01$ TNF α versus PBS for the same cell line in *F*.

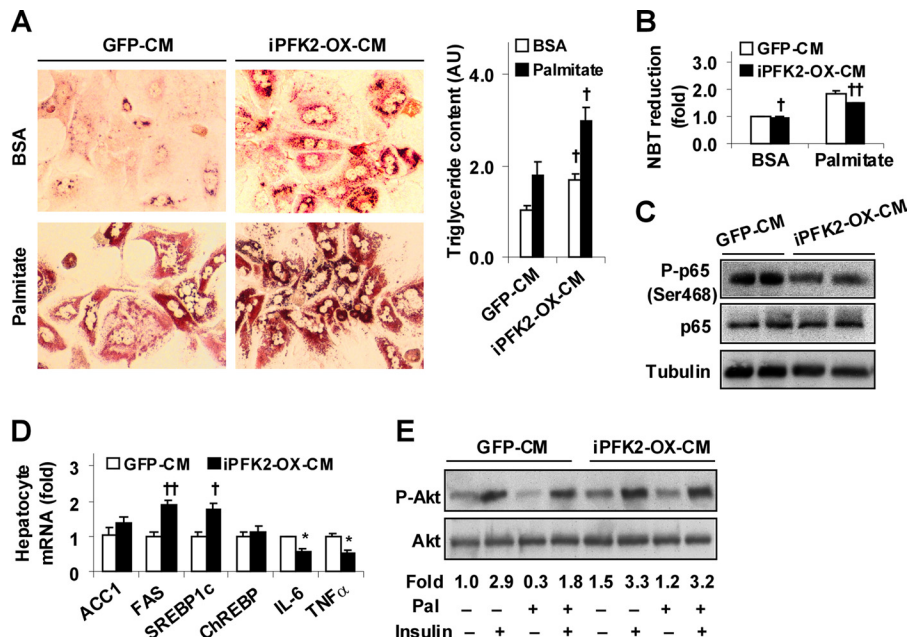


FIGURE 6. Adipocyte factors generated in response PFKFB3/iPFK2 overexpression decrease hepatocyte inflammatory response and improve insulin signaling while increasing hepatocyte fat deposition. Wild-type mouse primary hepatocytes were treated with adipocyte-CM in M199 medium at a 1:1 ratio for 48 h in the presence or absence of supplemental palmitate (250 μ M) for the last 24 h. Each of the assays was performed at least in quadruplicate. *A*, adipocyte-CM-treated mouse primary hepatocytes were stained with Oil Red O for 1 h (*left four panels*) and/or subjected to quantification of triglyceride content (*right panel*). AU, arbitrary unit. *B*, hepatocyte ROS production. *C*, hepatocyte levels of NF- κ B p65 and phospho-p65 (Ser-468). *D*, hepatocyte gene expression. *E*, hepatocyte insulin signaling. *A*, *B*, and *D*, numeric data are means \pm S.E. †, $p < 0.05$; ††, $p < 0.01$ iPFK2-OX-CM versus GFP-CM under the same condition (palmitate or BSA in *A* and *B*) and for the same gene (*D*). *E*, hepatocytes were incubated with or without insulin (100 nM) for 30 min prior to harvest. Phospho-Akt (Ser-473) to Akt1/2 ratios were calculated using densitometry and expressed as fold changes. *Pal*, palmitate.

iPKF2-overexpressing adipocytes in a manner that is anti-inflammatory and pro-lipogenic (see below and Refs. 15, 32). Considering this, by altering lipid composition, PFKFB3/iPKF2 may dissociate adipose tissue/adipocyte fat deposition and the inflammatory response. When the inflammatory response was decreased, insulin signaling through Akt was improved in both adipose tissue of Tg mice and in PFKFB3/iPKF2-overexpressing adipocytes. These results further support a role for PFKFB3/iPKF2 in regulating adipose tissue/adipocyte insulin sensitivity in a manner dependent on the inflammatory status but not fat deposition (20).

It also is a significant finding that in HFD-fed Tg mice the degree of hepatic steatosis was greater, whereas the severity of liver proinflammatory status and insulin resistance was lesser than in controls. This distal dissociation is consistent with liver phenotypes reported in mice in which the liver selectively overexpresses human diacylglycerol acyltransferase (15) and in mice that are treated with adenovirus to overexpress mCPT1a (16). However, unlike the two studies in which the liver originates metabolic alternations (15, 16), the aP2-PFKFB3 approach of this study suggests that adipose tissue initiated a dissociation of fat deposition and the inflammatory response, and the liver responded in a similar pattern. As substantial evidence, treatment of mouse primary hepatocytes with conditioned medium of PFKFB3/iPKF2-overexpressing adipocytes recapitulated liver phenotypes observed in HFD-fed Tg mice. Of importance, palmitoleate levels were increased in conditioned medium of PFKFB3/iPKF2-overexpressing adipocytes. Palmitoleate was initially thought to be anti-lipogenic (37). However, treatment of Huh7 hepatocytes with palmitoleate increased steatosis but decreased the phosphorylation of JNK1/2 (32). Furthermore, in this study, treatment of mouse primary hepatocytes with conditioned medium of PFKFB3/iPKF2-overexpressing adipocytes increased fat deposition but decreased hepatocyte ROS production, NF- κ B p65 phosphorylation, and proinflammatory cytokine expression. Given this, the composition of fat deposited but not fat content appears to control the status of hepatic inflammatory response. In terms of cross-talk between adipose and liver tissues, selective PFKFB3/iPKF2 overexpression appears to alter the adipose tissue lipid profile in a manner to cause a local dissociation of fat deposition and the inflammatory response. Meanwhile, the unique property of adipose tissue lipid profile was conveyed through the circulation and resulted in a similar change in liver lipid profile. The latter in turn accounted for, at least in part, a distal dissociation of hepatic steatosis and the inflammatory response. In this paradigm, the role of PFKFB3/iPKF2 is largely attributed to increasing adipocyte production of palmitoleate. In agreement with the inverse correlation between the status of proinflammatory response and insulin sensitivity observed in adipose tissue of this study and as reported elsewhere (15, 16, 31), HFD-fed Tg mice showed improvement in liver insulin sensitivity. Given an increase in liver fat deposition in HFD-Tg mice, hepatic steatosis is thus not necessarily a result of insulin resistance.

In the presence of a similar decrease in the status of proinflammatory response, macrophage numbers were increased in adipose tissue but decreased in livers in Tg mice compared with

control mice in response to HFD feeding. This is an interesting observation for which the underlying mechanisms remain to be explored. Nonetheless, similarities in adipose tissue inflammatory events between HFD-fed Tg mice and HFD-fed and rosiglitazone-treated wild-type mice (14, 21) suggest that adipose tissue macrophages in Tg mice were less activated in terms of their proinflammatory status. A possible explanation is that adipocyte factors generated in response to PFKFB3/iPKF2 overexpression suppressed macrophage proinflammatory response in a manner similar to that was observed in hepatocytes treated with adipocyte-conditioned medium. Another possible explanation is that PFKFB3/iPKF2 overexpression also occurred in macrophages and suppressed macrophage proinflammatory status as did PFKFB3/iPKF2 in adipocytes. At this point, a direct role for the PFKFB3/iPKF2 in macrophages in regulating macrophage inflammatory status is under investigation.

In summary, this study provides evidence to support a unique role for the PFKFB3/iPKF2 in adipocytes in dissociating inflammatory responses in both adipose and liver tissues following diet-induced fat deposition. Mechanistically, PFKFB3/iPKF2 enhances adipocyte glycolysis and glycolysis-derived lipogenesis, thereby generating a unique lipid profile that is characterized by increased levels of palmitoleate. These events contribute to both anti-inflammatory and insulin-sensitizing outcomes in adipose and liver tissues. As such, *PFKFB3* is likely a gene that promotes "healthy obesity."

REFERENCES

- Xu, H., Barnes, G. T., Yang, Q., Tan, G., Yang, D., Chou, C. J., Sole, J., Nichols, A., Ross, J. S., Tartaglia, L. A., and Chen, H. (2003) Chronic inflammation in fat plays a crucial role in the development of obesity-related insulin resistance. *J. Clin. Invest.* **112**, 1821–1830
- Tilig, H., and Hotamisligil, G. S. (2006) Nonalcoholic fatty liver disease. Cytokine-adipokine interplay and regulation of insulin resistance. *Gastroenterology* **131**, 934–945
- Menghini, R., Menini, S., Amoroso, R., Fiorentino, L., Casagrande, V., Marzano, V., Tornei, F., Bertucci, P., Iacobini, C., Serino, M., Porzio, O., Hribal, M. L., Folli, F., Khokha, R., Urbani, A., Lauro, R., Pugliese, G., and Federici, M. (2009) Tissue inhibitor of metalloproteinase 3 deficiency causes hepatic steatosis and adipose tissue inflammation in mice. *Gastroenterology* **136**, 663–672
- Iozzo, P., Bucci, M., Roivainen, A., Nägren, K., Järvisalo, M. J., Kiss, J., Guiducci, L., Fielding, B., Naum, A. G., Borra, R., Virtanen, K., Savunen, T., Salvadori, P. A., Ferrannini, E., Knuuti, J., and Nuutila, P. (2010) Fatty acid metabolism in the liver, measured by positron emission tomography, is increased in obese individuals. *Gastroenterology* **139**, 846–856
- Xu, A., Wang, Y., Keshaw, H., Xu, L. Y., Lam, K. S., and Cooper, G. J. (2003) The fat-derived hormone adiponectin alleviates alcoholic and nonalcoholic fatty liver diseases in mice. *J. Clin. Invest.* **112**, 91–100
- Weisberg, S. P., McCann, D., Desai, M., Rosenbaum, M., Leibel, R. L., and Ferrante, A. W., Jr. (2003) Obesity is associated with macrophage accumulation in adipose tissue. *J. Clin. Invest.* **112**, 1796–1808
- Joshi-Barve, S., Barve, S. S., Amancherla, K., Gobejishvili, L., Hill, D., Cave, M., Hote, P., and McClain, C. J. (2007) Palmitic acid induces production of proinflammatory cytokine interleukin-8 from hepatocytes. *Hepatology* **46**, 823–830
- Nakamura, S., Takamura, T., Matsuzawa-Nagata, N., Takayama, H., Misu, H., Noda, H., Nabemoto, S., Kurita, S., Ota, T., Ando, H., Miyamoto, K., and Kaneko, S. (2009) Palmitate induces insulin resistance in H4IIEC3 hepatocytes through reactive oxygen species produced by mitochondria. *J. Biol. Chem.* **284**, 14809–14818
- Samuel, V. T., Liu, Z. X., Qu, X., Elder, B. D., Bilz, S., Befroy, D., Romanelli,

Adipocyte iPFK2 Dissociates Inflammation from Fat Deposition

- A. J., and Shulman, G. I. (2004) Mechanism of hepatic insulin resistance in nonalcoholic fatty liver disease. *J. Biol. Chem.* **279**, 32345–32353
10. Samuel, V. T., Liu, Z. X., Wang, A., Beddow, S. A., Geisler, J. G., Kahn, M., Zhang, X. M., Monia, B. P., Bhanot, S., and Shulman, G. I. (2007) Inhibition of protein kinase C ϵ prevents hepatic insulin resistance in nonalcoholic fatty liver disease. *J. Clin. Invest.* **117**, 739–745
 11. Kang, K., Reilly, S. M., Karabacak, V., Gangl, M. R., Fitzgerald, K., Hatano, B., and Lee, C. H. (2008) Adipocyte-derived Th2 cytokines and myeloid PPAR δ regulate macrophage polarization and insulin sensitivity. *Cell Metab.* **7**, 485–495
 12. Odegaard, J. I., Ricardo-Gonzalez, R. R., Red Eagle, A., Vats, D., Morel, C. R., Goforth, M. H., Subramanian, V., Mukundan, L., Ferrante, A. W., and Chawla, A. (2008) Alternative M2 activation of Kupffer cells by PPAR δ ameliorates obesity-induced insulin resistance. *Cell Metab.* **7**, 496–507
 13. Combs, T. P., Pajvani, U. B., Berg, A. H., Lin, Y., Jelicks, L. A., Laplante, M., Nawrocki, A. R., Rajala, M. W., Parlow, A. F., Cheeseboro, L., Ding, Y. Y., Russell, R. G., Lindemann, D., Hartley, A., Baker, G. R., Obici, S., Deshaies, Y., Ludgate, M., Rossetti, L., and Scherer, P. E. (2004) A transgenic mouse with a deletion in the collagenous domain of adiponectin displays elevated circulating adiponectin and improved insulin sensitivity. *Endocrinology* **145**, 367–383
 14. Stienstra, R., Duval, C., Keshtkar, S., van der Laak, J., Kersten, S., and Müller, M. (2008) Peroxisome proliferator-activated receptor γ activation promotes infiltration of alternatively activated macrophages into adipose tissue. *J. Biol. Chem.* **283**, 22620–22627
 15. Monetti, M., Levin, M. C., Watt, M. J., Sajjan, M. P., Marmor, S., Hubbard, B. K., Stevens, R. D., Bain, J. R., Newgard, C. B., Farese, R. V., Sr., Hevener, A. L., and Farese, R. V., Jr. (2007) Dissociation of hepatic steatosis and insulin resistance in mice overexpressing DGAT in the liver. *Cell Metab.* **6**, 69–78
 16. Monsénégó, J., Mansouri, A., Akkaoui, M., Lenoir, V., Esnous, C., Fauveau, V., Tavernier, V., Girard, J., and Prip-Buus, C. (2012) Enhancing liver mitochondrial fatty acid oxidation capacity in obese mice improves insulin sensitivity independently of hepatic steatosis. *J. Hepatol.* **56**, 632–639
 17. Atsumi, T., Nishio, T., Niwa, H., Takeuchi, J., Bando, H., Shimizu, C., Yoshioka, N., Bucala, R., and Koike, T. (2005) Expression of inducible 6-phosphofructo-2-kinase/fructose-2,6-bisphosphatase/PPKFB3 isoforms in adipocytes and their potential role in glycolytic regulation. *Diabetes* **54**, 3349–3357
 18. Okar, D. A., Wu, C., and Lange, A. J. (2004) Regulation of the regulatory enzyme, 6-phosphofructo-2-kinase/fructose-2,6-bisphosphatase. *Adv. Enzyme Regul.* **44**, 123–154
 19. Rider, M. H., Bertrand, L., Vertommen, D., Michels, P. A., Rousseau, G. G., and Hue, L. (2004) 6-Phosphofructo-2-kinase/fructose-2,6-bisphosphatase. Head-to-head with a bifunctional enzyme that controls glycolysis. *Biochem. J.* **381**, 561–579
 20. Huo, Y., Guo, X., Li, H., Wang, H., Zhang, W., Wang, Y., Zhou, H., Gao, Z., Telang, S., Chesney, J., Chen, Y. E., Ye, J., Chapkin, R. S., and Wu, C. (2010) Disruption of inducible 6-phosphofructo-2-kinase ameliorates diet-induced adiposity but exacerbates systemic insulin resistance and adipose tissue inflammatory response. *J. Biol. Chem.* **285**, 3713–3721
 21. Guo, X., Xu, K., Zhang, J., Li, H., Zhang, W., Wang, H., Lange, A. J., Chen, Y. E., Huo, Y., and Wu, C. (2010) Involvement of inducible 6-phosphofructo-2-kinase in the anti-diabetic effect of peroxisome proliferator-activated receptor γ activation in mice. *J. Biol. Chem.* **285**, 23711–23720
 22. Minokoshi, Y., Kahn, C. R., and Kahn, B. B. (2003) Tissue-specific ablation of the GLUT4 glucose transporter or the insulin receptor challenges assumptions about insulin action and glucose homeostasis. *J. Biol. Chem.* **278**, 33609–33612
 23. Sugii, S., Olson, P., Sears, D. D., Saberi, M., Atkins, A. R., Barish, G. D., Hong, S. H., Castro, G. L., Yin, Y. Q., Nelson, M. C., Hsiao, G., Greaves, D. R., Downes, M., Yu, R. T., Olefsky, J. M., and Evans, R. M. (2009) PPAR γ activation in adipocytes is sufficient for systemic insulin sensitization. *Proc. Natl. Acad. Sci. U.S.A.* **106**, 22504–22509
 24. Wu, C., Okar, D. A., Newgard, C. B., and Lange, A. J. (2001) Overexpression of 6-phosphofructo-2-kinase/fructose-2,6-bisphosphatase in mouse liver lowers blood glucose by suppressing hepatic glucose production. *J. Clin. Invest.* **107**, 91–98
 25. Wu, C., Kang, J. E., Peng, L. J., Li, H., Khan, S. A., Hillard, C. J., Okar, D. A., and Lange, A. J. (2005) Enhancing hepatic glycolysis reduces obesity. Differential effects on lipogenesis depend on site of glycolytic modulation. *Cell Metab.* **2**, 131–140
 26. Wu, C., Khan, S. A., Peng, L. J., Li, H., Carmella, S. G., and Lange, A. J. (2006) Perturbation of glucose flux in the liver by decreasing F26P2 levels causes hepatic insulin resistance and hyperglycemia. *Am. J. Physiol. Endocrinol. Metab.* **291**, E536–E543
 27. Kamagate, A., Qu, S., Perdomo, G., Su, D., Kim, D. H., Slusher, S., Meseck, M., and Dong, H. H. (2008) FoxO1 mediates insulin-dependent regulation of hepatic VLDL production in mice. *J. Clin. Invest.* **118**, 2347–2364
 28. Bu, S. Y., Mashek, M. T., and Mashek, D. G. (2009) Suppression of long chain acyl-CoA synthetase 3 decreases hepatic *de novo* fatty acid synthesis through decreased transcriptional activity. *J. Biol. Chem.* **284**, 30474–30483
 29. Chapkin, R. S., and Carmichael, S. L. (1990) Effects of dietary *n*-3 and *n*-6 polyunsaturated fatty acids on macrophage phospholipid classes and subclasses. *Lipids* **25**, 827–834
 30. Lesniewski, L. A., Hosch, S. E., Neels, J. G., de Luca, C., Pashmforoush, M., Lumeng, C. N., Chiang, S. H., Scadeng, M., Saltiel, A. R., and Olefsky, J. M. (2007) Bone marrow-specific Cap gene deletion protects against high fat diet-induced insulin resistance. *Nat. Med.* **13**, 455–462
 31. Cai, D., Yuan, M., Frantz, D. F., Melendez, P. A., Hansen, L., Lee, J., and Shoelson, S. E. (2005) Local and systemic insulin resistance resulting from hepatic activation of IKK- β and NF- κ B. *Nat. Med.* **11**, 183–190
 32. Akazawa, Y., Cazanave, S., Mott, J. L., Elmi, N., Bronk, S. F., Kohno, S., Charlton, M. R., and Gores, G. J. (2010) Palmitoleate attenuates palmitate-induced Bim and PUMA up-regulation and hepatocyte lipopoptosis. *J. Hepatol.* **52**, 586–593
 33. Clément, S., Juge-Aubry, C., Sgroi, A., Conzelmann, S., Paziienza, V., Pittet-Cuenod, B., Meier, C. A., and Negro, F. (2008) Monocyte chemoattractant protein-1 secreted by adipose tissue induces direct lipid accumulation in hepatocytes. *Hepatology* **48**, 799–807
 34. Liu, X., Miyazaki, M., Flowers, M. T., Sampath, H., Zhao, M., Chu, K., Paton, C. M., Joo, D. S., and Ntambi, J. M. (2010) Loss of stearoyl-CoA desaturase-1 attenuates adipocyte inflammation. Effects of adipocyte-derived oleate. *Arterioscler. Thromb. Vasc. Biol.* **30**, 31–38
 35. Zhang, J., Fu, M., Cui, T., Xiong, C., Xu, K., Zhong, W., Xiao, Y., Floyd, D., Liang, J., Li, E., Song, Q., and Chen, Y. E. (2004) Selective disruption of PPAR γ 2 impairs the development of adipose tissue and insulin sensitivity. *Proc. Natl. Acad. Sci. U.S.A.* **101**, 10703–10708
 36. Kamei, N., Tobe, K., Suzuki, R., Ohsugi, M., Watanabe, T., Kubota, N., Ohtsuka-Kawatari, N., Kumagai, K., Sakamoto, K., Kobayashi, M., Yamachi, T., Ueki, K., Oishi, Y., Nishimura, S., Manabe, I., Hashimoto, H., Ohnishi, Y., Ogata, H., Tokuyama, K., Tsunoda, M., Ide, T., Murakami, K., Nagai, R., and Kadowaki, T. (2006) Overexpression of monocyte chemoattractant protein-1 in adipose tissues causes macrophage recruitment and insulin resistance. *J. Biol. Chem.* **281**, 26602–26614
 37. Cao, H., Gerhold, K., Mayers, J. R., Wiest, M. M., Watkins, S. M., and Hotamisligil, G. S. (2008) Identification of a lipokine, a lipid hormone linking adipose tissue to systemic metabolism. *Cell* **134**, 933–944